CrystEngComm

Crystal Growth, Structural Characterization, Cation-Cation Classification, and Optical Properties of Uranium(VI) Containing Oxychlorides, A4U5O16Cl2 (A = K, Rb), Cs5U7O22Cl3, and AUO3Cl (A = Rb, Cs)

Journal:	*CrystEngComm*
Manuscript ID:	CE-ART-02-2014-000281.R1
Article Type:	Paper
Date Submitted by the Author:	20-Mar-2014
Complete List of Authors:	Read, Cory; University of South Carolina, Chemistry and Biochemistry Yeon, Yeongho; University of South Carolina, Chemistry and Biochemistry Smith, Mark; University of South Carolina, Department of Chemistry and Biochemistry Zur Loye, Hans-Conrad; University of South Carolina, Department of Chemistry and Biochemistry

Crystal Growth, Structural Characterization, Cation-Cation Classification, and Optical Properties of Uranium(VI) Containing Oxychlorides, $A_4U_5O_{16}Cl_2$ (*A* = K, Rb), $Cs_5U_7O_{22}Cl_3$, and AUO_3Cl (*A* = Rb, Cs)

Cory Michael Read,[1] *Jeongho Yeon,*[1] *Mark D. Smith,*[1] *and Hans-Conrad zur Loye,*[1*]

[1]Department of Chemistry and Biochemistry, University of South Carolina, Columbia, SC 29208

Corresponding Authors: *E-mail: zurloye@mailbox.sc.edu

RECEIVED DATE (to be automatically inserted after your manuscript is accepted if required according to the journal that you are submitting your paper to)

Crystal Growth, Structural Characterization, Cation-Cation Classification, and Optical Properties of Uranium(VI) Containing Oxychlorides, $A_4U_5O_{16}Cl_2$ (*A* = K, Rb), $Cs_5U_7O_{22}Cl_3$, and AUO_3Cl (*A* = Rb, Cs)

Cory Michael Read,[1] Jeongho Yeon,[1] Mark D. Smith,[1] and Hans-Conrad zur Loye,[1]*

[1]Department of Chemistry and Biochemistry, University of South Carolina, Columbia, SC 29208

Table of Contents Abstract

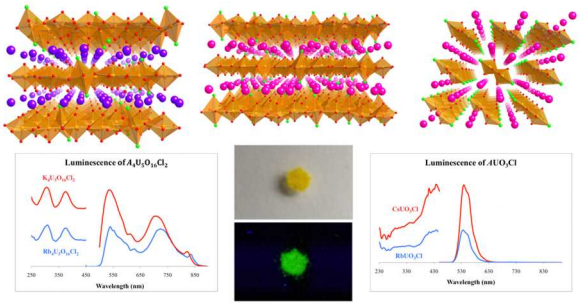

Single crystals of five new oxychlorides, $K_4U_5O_{16}Cl_2$, $Rb_4U_5O_{16}Cl_2$, $Cs_5U_7O_{22}Cl_3$, $RbUO_3Cl$, and $CsUO_3Cl$, grown from molten chloride fluxes. Compounds exhibit novel layer topology, cation-cation interactions, or chain structures and are luminescent. CCI's were classified according to a generalized CCI classification for actinyl ions presented in the paper.

Crystal Growth, Structural Characterization, Cation-Cation Classification, and Optical Properties of Uranium(VI) Containing Oxychlorides, $A_4U_5O_{16}Cl_2$ (*A* = K, Rb), $Cs_5U_7O_{22}Cl_3$, and AUO_3Cl (*A* = Rb, Cs)

Cory Michael Read,[1] Jeongho Yeon,[1] Mark D. Smith,[1] and Hans-Conrad zur Loye,[1]*

[1]Department of Chemistry and Biochemistry, University of South Carolina, Columbia, SC 29208

Abstract

Single crystals of five new alkali metal uranium oxychlorides, $K_4U_5O_{16}Cl_2$, $Rb_4U_5O_{16}Cl_2$, $Cs_5U_7O_{22}Cl_3$, $RbUO_3Cl$, and $CsUO_3Cl$, have been grown from molten chloride fluxes and structurally characterized by single crystal X-ray diffraction. All of the materials are monoclinic. The first three crystallize in the space group $P2_1/n$ and exhibit a 2D layered structure with a novel layer topology, consisting of UO_6, UO_7, and UO_4Cl_2 polyhedra and cation-cation interactions (CCIs) within the plane of the uranyl sheet. A general Cation-Cation Classification scheme is presented. $RbUO_3Cl$ and $CsUO_3Cl$ crystallize in the space group $P2_1/m$ and exhibit 1D zipper-like chains of UO_5Cl_2 polyhedra. The lattice parameters of the new oxychlorides are: $K_4U_5O_{16}Cl_2$, a = 9.9574(4) Å, b = 6.9766(3) Å, c = 14.3920(6) Å, and β = 105.7690(10)°; $Rb_4U_5O_{16}Cl_2$, a = 10.2164(4) Å, b = 7.0160(3) Å, c = 14.4930(5) Å, and β = 103.8290(10)°; $Cs_5U_7O_{22}Cl_3$, a = 10.6214(5) Å, b = 18.1071(8) Å, c = 16.0857(7) Å, and β = 102.9850(10)°; $RbUO_3Cl$, a = 7.3602(6) Å, b = 4.1127(3) Å, c = 8.5556(7) Å, and β = 104.602(2)°; $CsUO_3Cl$, a = 7.7768(4) Å, b = 4.1245(2) Å, c = 8.7701(5) Å, and β = 105.4680(10)°. The materials were further characterized by UV-Vis reflectance spectroscopy and fluorescence spectroscopy.

Introduction

The chemistry of uranium in extended structures has been extensively investigated due to its importance for long term nuclear waste storage and the development of fuel rod assemblies. In recent years, several research groups have focused on elucidating the chemical and structural complexities that uranium can adopt. As a result of their efforts, single crystals of many new compounds, including hybrid materials[1], nitrite complexes[2], phosphates[3], borates[4], oxychlorides[5], and silicates[6] have been grown and structurally characterized.

The flux crystal growth technique has been used successfully by a number of groups to obtain single crystals of many uranium containing oxide materials.[7-11] We have used hydroxide or carbonate fluxes, which have resulted in several oxides, many of which belong to previously known structure types.[12-16] Hydroxide fluxes, however, tend to primarily promote the crystallization of simple ternary alkali metal uranium oxides. Carbonate melts, on the other hand, have been quite successful for the growth of more complex compositions, many of which have taken on perovskite-type structures. Reports in the literature indicate that some uranium containing oxides, as well as related materials, such as $K_6(UO_2)_5(VO_4)_2O_5$[17], $K_4[(UO_2)_5(TeO_3)_2O_5]$[18], and $A_7(UO_2)_8(VO_4)_2O_8Cl$ (A = Rb, Cs)[5], can be synthesized from alkali metal chloride fluxes. In an effort to expand the library of known uranium oxides and oxychlorides, we decided to further explore the use of halide fluxes.

The literature describing compounds containing uranium(VI) is dominated by one main structural feature, the uranyl cation, UO_2^{2+}, which exhibits distorted square-, pentagonal-, or hexagonal-bipyramidal coordination environments with the corresponding bonding motif of two short axial bonds and four, five, or six long equatorial bonds. The short axial bonded oxygen atoms are most often terminal, while the ligands bound in the equatorial position can participate

in further bonding. Uranium-containing oxychlorides are no exception and also contain uranyl cations; however, to date, only a small number of reports describing structurally characterized oxychlorides have appeared in the literature. The majority of the materials in this class contain uranium(VI), all of which contain UO_2^{2+}. The known compounds are based on isolated polyhedra[19], finite clusters[20], chains[21], sheets[5], and frameworks[22] of uranyl polyhedra. The bulk of these known structures are composed of isolated polyhedra or finite clusters.

The axial oxide ligands in AnO_2^{2+} (*An* = actinide) are most often terminal, not exhibiting further bonding to other *An* centers. This latter type of bonding arrangement between actinide centers is referred to as a cation-cation interaction (CCI), and is much more common in AnO_2^{+} compounds, because the axial *An*-O bonds are slightly weaker with the pentavalent actinide. First observed in solution,[23] the CCI has since been investigated in several solid state compounds, amounting to about fifty percent of NpO_2^{+} compositions but only approximately two percent of UO_2^{2+} inorganic compounds.[24, 25] For a CCI to occur between uranyl centers, the uranyl bond valence has to decrease, thereby lengthening the U-O distance. A classification scheme for observed NpO_2^{+} CCIs was developed in 2004, providing eight generalized binding motifs.[26] The classification scheme was later updated for UO_2^{2+}, displaying seven distinct binding modes for observed uranyl CCIs, including both two- and three-centered CCIs.[27] Herein, we present a more generalized classification that includes both two- and three-centered CCIs, and would be applicable to currently unobserved interactions, shown in Scheme 1. The uranyl oxygen can participate in two- and three-centered CCIs, allowing for five different uranyl donor combinations. A uranyl ion can accept a uranyl oxygen in an equatorial bond with or without donating its uranyl oxygen. A uranyl that accepts, but does not donate, presents the sixth possibility. The number of uranyl acceptors can be 0, 1, 2, …, presumably up to 5. A

comprehensive table of possible combinations is given in Table S1, which should hold true for any actinyl compound. UO_2Cl_2[22] is the only reported example of a uranium oxychloride having CCIs. We present, in this manuscript, three new uranyl oxychlorides, $K_4U_5O_{16}Cl_2$, $Rb_4U_5O_{16}Cl_2$, and $Cs_5U_7O_{22}Cl_3$, displaying CCIs and classify them according to our general classification scheme.

The synthesis, characterization, and optical properties of five novel oxychlorides with compositions $A_4U_5O_{16}Cl_2$ (A = K, Rb), $Cs_5U_7O_{22}Cl_3$, and AUO_3Cl (A = Cs, Rb) are reported herein.

Experimental Section

Reagents. UO_3 (International Bioanalitics Industries Inc.), U_3O_8 (International Bioanalitics Industries Inc., ACS grade), $MnCl_2$•$4H_2O$ (Alfa Aesar, 99%), KCl (Mallinckrodt, ACS grade), RbCl (Alfa Aesar, 99%), and CsCl (Alfa Aesar, 99%) were used as received.

Synthesis. Single crystals of the title materials were grown from molten chloride fluxes.

For the preparation of $K_4U_5O_{16}Cl_2$ (**1**), $Rb_4U_5O_{16}Cl_2$ (**2**), $RbUO_3Cl$ (**4**), and $CsUO_3Cl$ (**5**), 1 mmol UO_3 and 20 mmol ACl (A = K, Rb, Cs) were added to a quartz tube that was sealed at one end. The tube was then heated to 160 °C in a vacuum oven at 700 mmHg vacuum and kept there for 3 days to dry the respective chloride. The tubes were then evacuated to approx. 10^{-4} mmHg, and flame sealed. The reactants were heated to 900 °C at a rate of 10 °C/min, allowed to dwell for 20 h, cooled to 550 °C at a rate of 0.1 °C/min, and finally cooled to room temperature by turning the furnace off. The flux was quickly washed away with water, aided by ultrasonication, and the crystals were isolated by vacuum filtration. The KCl reaction yielded a single phase of orange $K_4U_5O_{16}Cl_2$ crystals, in approximately 90% yield based on U. The RbCl reaction produced an approximately 50/50 mixture of large, orange $Rb_4U_5O_{16}Cl_2$ crystals and small,

yellow $RbUO_3Cl$ crystals, which were manually separated. The CsCl reaction resulted in the formation of both $CsUO_3Cl$ and $Cs_2U_4O_{13}$, a previously known oxide[28]. The red-orange $Cs_2U_4O_{13}$ crystals grew on the side of the reaction tube near the top, while the yellow $CsUO_3Cl$ crystals formed in the bottom of the tube, allowing for easy separation.

For the preparation of $Cs_5U_7O_{22}Cl_3$ (**3**), 1 mmol U_3O_8, 2 mmol $MnCl_2 \cdot 4H_2O$, and 40 mmol CsCl were added to an alumina crucible and covered with an alumina disc. The charge was heated to 900 °C at a rate of 10 °C/min, allowed to dwell for 12 h, cooled to 550 °C at a rate of 0.1 °C/min, and finally cooled to room temperature by turning the furnace off. The small orange plate crystals were a very minor phase and had an irregular shape, with rounded corners and edges suggesting partial dissolution in the melt after crystal growth. The significance of the transition metal in the reaction melt, although essential for crystal formation, is unclear, and all attempts to synthesize a phase pure sample were unsuccessful.

Single Crystal X–ray Diffraction.

X-ray intensity data from plate-like crystals of **1**, **2**, and **3** and needle crystals of **4** and **5** were collected at 296(2) K using a Bruker SMART APEX diffractometer (Mo Kα radiation, λ = 0.71073 Å).[29] The data collection covered 100% of reciprocal space to $2\theta_{max}$ = 60.6-70.5º, with average reflection redundancy of 5.6-8.3, and R_{int} = 0.0374-0.107 after absorption correction. The raw area detector data frames were reduced and corrected for absorption effects with the SAINT+ and SADABS programs.[29] Final unit cell parameters were determined by least-squares refinements. Direct methods structure solution, difference Fourier calculations and full-matrix least-squares refinement against F^2 were performed with SHELXS/L[30] as implemented in OLEX2[31] for **1**-**3** and with SHELXL-2013/4[30] using the ShelXle interface[32] for **4** and **5**. Crystallographic data for the title compounds can be found in Table 1 and Table 2.

Some difficulty was encountered in finding a suitable crystal for **4** and **5**, as most specimens were visibly twinned and did not cleave favorably. Eventually small crystals were selected and used for the data collections. After location and anisotropic refinement of all atomic positions of **5**, a pattern of $F_{obs}>>F_{calc}$ was observed for reflections with the worst data/model agreement, suggesting twinning. Analysis of the F_{obs}/F_{calc} pattern using the TwinRotMat program in PLATON[33] found a minor twin domain related to the primary domain by a two-fold axis perpendicular to (001), with an estimated contribution of 0.08. This was not detected during pre-data collection crystal screening. The derived twin law is, by rows, [-1 0 0 / 0 -1 0 / 0.602 0 1]. TwinRotMat was used to generate an SHELX HKLF5 format reflection file in which 225 of the 1105 total reflections are overlapped and contain contributions from the both twin domains. Accounting for this minor non-merohedral twinning in the refinement reduced the $R1$-values from 0.037 to 0.026, and flattened the residual electron density map from $\Delta\rho$(max/min) = +3.74/-3.69 to +1.56/-1.67 e Å^{-3}. The volume of the minor twin domain refined to 0.079(2). No deviation from full occupancy was observed for the uranium, cesium or chlorine atoms. Trial refinements of the site occupancy parameters for these atoms resulted in U, 0.99(1); Cs, 1.01(1), Cl, 1.00(1). Analysis of the F_{obs}/F_{calc} pattern in **4** showed no evidence for unidentified non-merohedral twinning. No deviation from full occupancy was observed for the uranium, rubidium or chlorine atoms. Trial refinements of the site occupancy parameters for these atoms resulted in U, 0.99(1); Rb, 1.01(1), Cl, 0.99(1). Final atomic coordinates were standardized with Structure Tidy.[33]

Powder X–ray Diffraction. Powder X-ray diffraction data were collected on a Rigaku D/Max-2100 powder X-ray diffractometer using Cu Kα radiation. The step-scan covered the

angular range 10-70° 2θ in steps of 0.04°. No impurities were observed, and the calculated and experimental PXRD patterns are in excellent agreement (See Figure S1- Figure S4).

Energy-Dispersive Spectroscopy (EDS). Elemental analysis was performed on the flux-grown crystals using a TESCAN Vega-3 SBU scanning electron microscope (SEM) with EDS capabilities. The crystals were mounted on carbon tape and analyzed using a 20 kV accelerating voltage and an accumulation time of 20 s. As a qualitative measure, the EDS confirmed the presence of each reported element in the title compounds.

Optical Spectroscopy. UV-Vis diffuse reflectance spectra of polycrystalline powder samples of the reported materials were obtained using a Perkin Elmer Lambda 35 UV/vis scanning spectrophotometer equipped with an integrating sphere in the range 200 – 900 nm. Luminescence spectra of polycrystalline powder samples of the reported materials were obtained using a Perkin Elmer LS-55 fluorescence spectrometer. Excitation and emission scans were performed in the 250 – 450 and 450 – 900 nm ranges, respectively.

Results and Discussion

Synthesis. Uranium oxychlorides have been synthesized by several different methods, including precipitation from low-temperature solutions, solid state processing, and flux crystal growth. The majority of the compositions were made from low-temperature solutions with high chloride concentrations,[19, 21, 34-36] however, like all methods, this approach has limitations and it will not crystallize structures where high temperatures are needed to overcome thermal barriers. The flux growth technique, on the other hand, has proven very effective for the discovery of new complex oxide materials,[37] and the use of chloride fluxes for the growth of uranium containing oxides and oxychlorides has been reported previously,[5, 17, 28, 38] suggesting great promise for discovery of novel oxychlorides. Reactions performed in chloride melts open to the air in rare

instances yield oxychloride products. However, it is possible to optimize the reaction conditions to make this process more deliberate for the discovery of new oxychloride materials. Specifically, by drying the reagents, especially the hygroscopic chloride fluxes, to remove any undesired water from the reaction, and by performing the crystal growth process in evacuated, flame-dried, sealed tubes it is possible to promote the formation of oxychlorides over oxides that would typically form in an open reaction system.

Structures. $A_4U_5O_{16}Cl_2$ (A = K, Rb) (**1** and **2**) are isostructural and crystallize in the monoclinic space group, $P2_1/n$. The two compounds exhibit an overall two-dimensional (2D) layered structure as seen in Figure 1. The uranium atoms reside in three crystallographically unique sites with UO_6, UO_7, and UO_4Cl_2 coordination environments. The $U(2)O_6$ and $U(1)O_7$ environments are distorted, having two short axial U-O bonds at 1.801(5)-1.828(5) Å, and four or five long equatorial U-O bonds ranging from 2.185(3)-2.540(4) Å, which is consistent with a typical uranyl bonding motif. The $U(3)O_4Cl_2$ environment has two U-O bonds at 1.869(4)-1.871(4) Å and two U-O bonds at 2.096(3)-2.104(4) Å, which is similar to those observed in the uranyl environments of tetraoxouranates.[39] The two U-Cl bonds are 2.6761(16)-2.7003(19) Å and are consistent with the average U-Cl bond length found in other uranium oxychlorides. The two tightly bound oxygen atoms of $U(3)O_4Cl_2$ polyhedra are corner-sharing in the equatorial position of the $U(1)O_7$ pentagonal bipyramids. The remaining oxygen atoms are each corner-sharing with two $U(2)O_6$ polyhedra, as seen in Figure 2. The $U(2)O_6$ and $U(1)O_7$ polyhedra only share oxygen atoms in the equatorial plane, as shown in Figure 2. The bond lengths for the uranium environments are listed in Table 3. The uranyl polyhedra are edge- and corner-sharing in the plane perpendicular to the [101] direction, creating a 2D sheet containing uranyl oxygen atoms while the chlorine atoms are located above and below the sheet as shown in Figure 3. A

very similar structural motif has been observed in two other compounds, $Pb_2[(UO_2)_5O_6(OH)_2](H_2O)_4$ [40] and $K_2U_7O_{22}$[41], that differ from **1** and **2** by having a UO_7 polyhedron rather than a UO_6 polyhedron. The uranyl sheets are separated by layers of alkali metal ions to balance the charge, forming the overall layered structure.

$Cs_5U_7O_{22}Cl_3$ (**3**) also crystallizes in the $P2_1/n$ space group. The structure is similar to that of $A_4U_5O_{16}Cl_2$ (A = K, Rb) in that it is a layered structure, comprised of uranyl sheets separated by alkali metal ions, as illustrated in Figure 4. The uranyl sheets, however, are composed of eight crystallographically unique sites, which exhibit one of three different binding motifs, UO_6, UO_7, or UO_4Cl_2. U(5) and U(8) are in UO_4Cl_2 coordination environments, U(7) is in a UO_6 coordination environment and the remaining five uranium atoms are in UO_7 coordination environments. The UO_4Cl_2 environments have respective axial and equatorial U-O bond lengths of 1.892(7)-1.960(7) and 2.003(6)-2.056(7) Å, which is closer to a uniform distribution of U-O bond lengths than found in $A_4U_5O_{16}Cl_2$, and different from a typical uranyl environment. Figure 5 highlights the different uranium environments, and the associated bond lengths are listed in Table 3. The uranyl polyhedra edge- and corner-share oxygen atoms to form the sheets shown in Figure 6. To our knowledge, this is the first reported structure containing sheets with this topology, adding to the diverse list of uranyl sheet topologies compiled by Burns in 2005.[42]

It is not typical for the uranyl oxygen atoms to participate in bonding interactions with other uranyl centers. When this phenomenon occurs it is referred to a cation-cation interaction (CCI). A typical interaction of this type has been observed in a small number of uranium(VI) materials,[27, 43-53] including $UO_2(NO_2TA)_2$-H_2O, where the uranyl oxide is bound in the equatorial position of a neighboring uranium atom.[54] The bond involved in the CCI is slightly longer than the remaining uranyl bonds in the structure. For a typical uranyl environment, the bond valence

sums for the axial and equatorial bonds are 4+ and 2+ respectively, for a net uranium valence of 6+. In $UO_2(NO_2TA)_2$-H_2O, the sums were 3.84 and 2.19 for the axial and equatorial bonds, respectively. This observed lowering of the axial bond valence is due to the oxygen forming longer bonds with both its primary and its neighboring uranium cation. In a typical uranyl layered structure without CCIs, the terminal oxo ligands are located above and below the plane of the sheet. The most interesting aspect of the structures of **1**-**3** involves the UO_4Cl_2 environments. Having terminal trans-oriented chlorides above and below the sheet structure forces the uranyl oxygen atoms to be in the plane of the sheet, directing them to bond to other uranium atoms, forming sterically mediated CCIs (see Figure 3a). U(3) donates each uranyl oxygen in a two-centered CCI to U(1), exhibiting Type **3** and Type **6** interactions, respectively. For **1** and **2**, the UO_4Cl_2 environment is somewhat different from the typical uranyl environment, having slightly longer uranyl bonds and slightly shorter equatorial U-O bonds with respective axial and equatorial bond valence sums of 2.84 and 2.89 for **1** and 2.83 and 2.80 for **2**. The uranyl oxo ligands are underbonded relative to what is found for the typical uranyl motif, presumably due to the presence of the CCI. Introducing a larger cation, Cs^+, between the layers further distorts the UO_4Cl_2 environment in the $Cs_5U_7O_{22}Cl_3$ structure. The U-O bonds have to adjust to accommodate this change in structure, creating even longer uranyl bonds and shorter equatorial U-O bonds. The calculated bond valence sums for the axial and equatorial bonds are 2.53 and 3.17 for U(5) and 2.72 and 2.97 for U(8), respectively. The further underbonded uranyl oxygen atoms in this structure are able to form additional connections and, thus, each is corner-sharing with two UO_7 polyhedra (see Figure 6). U(5) donates each uranyl oxygen in three-centered CCIs, one with U(1) and U(6) and one with two U(3) centers, which are corner-sharing with an additional U(5) uranyl. U(5), U(1) and U(6), and U(3) exhibit Type **5**, **6**, and **12** CCIs,

respectively. U(8) also donates both uranyl oxygen atoms in three-centered CCIs to U(2) and U(4) on each side, displaying Type **5** and **6** CCIs, respectively.

AUO$_3$Cl (A = Rb, Cs) are isostructural, and crystallize in the monoclinic space group, $P2_1/m$. A related compound was reported by Allpress in 1964, $Cs_{0.9}(UO_2)OCl_{0.9}$, having a very similar crystal structure, however, with an unexpected fractional occupancy of the Cs and Cl sites.[38] **4** and **5** exhibit a one-dimensional chain-type structure overall, as seen in Figure 7. There is one single uranium site, which has a UO_5Cl_2 pentagonal bipyramidal arrangement shown in Figure 8a with the associated bond lengths listed in Table 4. There are two short U-O axial bonds ranging from 1.802(6)-1.824(8) Å and three long U-O equatorial bonds ranging from 2.211(3)-2.268(6) Å, consistent with the uranyl environment. The two equatorial U-Cl bonds at 2.974(2) and 2.9817(14) Å are long, and represent the upper limit for U-Cl bond lengths in uranium oxychlorides; however, it is not uncommon for bridging halides to exhibit long bond distances.[55-57] The uranium polyhedra share four of the five equatorial edges to create a zipper-like uranyl chain illustrated in Figure 8b. The uranyl oxo ligands are oriented out of the plane of the zipper, preventing the formation of CCIs.

The bond valence sums for all the uranium atoms have been calculated for **1-5**, and are listed in Table 5. The optimized parameters provided by Burns,[58] r_{U-O} = 2.051 and b = 0.519, were used for calculating the U-O valences, and the parameters provided by Zachariesen,[59] r_{U-Cl} = 2.420 and b = 0.4 , were used for calculating U-Cl valences. The BVS values of 5.63-6.07 are all in agreement with uranium in the +6 oxidation state.

Optical Spectroscopy. UV-vis diffuse reflectance data were measured on ground crystals of **1**, **2**, **4**, and **5**, and converted to absorbance vs. wavelength plots using the Kubelka-Munk function.[60] All compounds displayed a broad absorption band covering from 200-570 nm (see

Figure S5). With an estimated band gap of 2.17-2.28 eV, these materials can be classified as semiconductors.

Luminescence data were also collected on ground crystals of **1**, **2**, **4**, and **5**. Compounds **1** and **2** are only weakly luminescent (see Figure 9) with λ_{max} = 537 and 536 nm, for λ_{ex} = 311 and 308 nm, respectively. Compounds **4** and **5** are strongly luminescent (see Figure 10) with λ_{max} = 535 and 539 nm, respectively, for λ_{ex} = 439 nm.

Conclusions

We have successfully synthesized and characterized five novel uranium oxychlorides, $K_4U_5O_{16}Cl_2$ (**1**), $Rb_4U_5O_{16}Cl_2$ (**2**), $Cs_5U_7O_{22}Cl_3$ (**3**), $RbUO_3Cl$ (**4**), and $CsUO_3Cl$ (**5**). The first three materials exhibit 2D layered structures with new uranyl sheet topologies containing cation-cation interactions, and **1** and **2** are weakly luminescent. Compounds **4** and **5** crystallize in 1D zipper-like chain structures, and exhibit strong luminescence. A new Cation-Cation Interaction Classification scheme is presented and the uranyl centers exhibiting CCIs were classified according to this general scheme.

Acknowledgments. Research was supported by the U.S. Department of Energy, Office of Basic Energy Sciences, Division of Materials Sciences and Engineering under Award DE-SC0008664.

Supporting Information. Powder XRD patterns, UV–vis spectra, and atomic coordinates and equivalent isotropic displacement parameters. Further details of the crystal structure investigation can be obtained from the Fachinformationszentrum Karlsruhe, 76344 Eggenstein-Leopoldshafen, Germany (fax: +497247808666; e-mail: crystdata@fiz-karlsruhe.de) on quoting

the depository numbers CSD-427327, CSD-427328, CSD-427329, CSD-427330, and CSD-427331.

References

1. M. B. Andrews and C. L. Cahill, *Angew. Chem. Int. Ed. Engl.*, 2012, **51**, 6631-6634.
2. F. Dulong, J. Pouessel, P. Thuery, J. C. Berthet, M. Ephritikhine and T. Cantat, *Chem. Commun.*, 2013, **49**, 2412-2414.
3. E. M. Villa, C. J. Marr, J. Diwu, E. V. Alekseev, W. Depmeier and T. E. Albrecht-Schmitt, *Inorg. Chem.*, 2013, **52**, 965-973.
4. S. Wu, S. Wang, M. Polinski, O. Beermann, P. Kegler, T. Malcherek, A. Holzheid, W. Depmeier, D. Bosbach, T. E. Albrecht-Schmitt and E. V. Alekseev, *Inorg. Chem.*, 2013, **52**, 5110-5118.
5. I. Duribreux, M. Saadi, S. Obbade, C. Dion and F. Abraham, *J. Solid State Chem.*, 2003, **172**, 351-363.
6. Y. C. Chang, W. J. Chang, S. Boudin and K. H. Lii, *Inorg. Chem.*, 2013, **52**, 7230-7235.
7. C. S. Lee, S. L. Wang, Y. H. Chen and K. H. Lii, *Inorg. Chem.*, 2009, **48**, 8357-8361.
8. S. P. Liu, M. L. Chen, B. C. Chang and K. H. Lii, *Inorg. Chem.*, 2013, **52**, 3990-3994.
9. S. Wang, E. V. Alekseev, W. Depmeier and T. E. Albrecht-Schmitt, *Chem. Commun.*, 2011, **47**, 10874-10885.
10. S. Wang, E. V. Alekseev, J. Diwu, H. M. Miller, A. G. Oliver, G. Liu, W. Depmeier and T. E. Albrecht-Schmitt, *Chem. Mater.*, 2011, **23**, 2931-2939.
11. S. Yagoubi, S. Obbade, S. Saad and F. Abraham, *J. Solid State Chem.*, 2011, **184**,

971-981.

12. C. M. Read, D. E. Bugaris and L. zur, Hans-Conrad, *Solid State Sci.*, 2013, **17**, 40-45.

13. C. M. Read, M. D. Smith and H.-C. Loye, *J. Chem. Crystallogr.*, 2013, **43**, 484-487.

14. I. P. Roof, M. D. Smith and H.-C. zur Loye, *J. Cryst. Growth*, 2010, **312**, 1240-1243.

15. I. P. Roof, M. D. Smith and H.-C. zur Loye, *Solid State Sci.*, 2010, **12**, 1941-1947.

16. I. P. Roof, M. D. Smith and H.-C. zur Loye, *J. Chem. Crystallogr.*, 2010, **40**, 491-495.

17. C. Dion, S. Obbade, E. Raekelboom, F. Abraham and M. Saadi, *J. Solid State Chem.*, 2000, **155**, 342-353.

18. J. D. Woodward and T. E. Albrecht-Schmitt, *J. Solid State Chem.*, 2005, **178**, 2922-2926.

19. D. J. Watkin, R. G. Denning and K. Prout, *Acta Crystallogr. C*, 1991, **47**, 2517-2519.

20. A. Perrin, *J. Applied Crystallogr.*, 1977, **10**, 360-361.

21. A. C. Bean, Y. Xu, J. A. Danis, T. E. Albrecht-Schmitt, B. L. Scott and W. Runde, *Inorg. Chem.*, 2002, **41**, 6775-6779.

22. J. C. Taylor and P. W. Wilson, *Acta Crystallogr. B*, 1973, **29**, 1073-1076.

23. J. C. Sullivan, J. C. Hindman and A. J. Zielen, *J. Am. Chem. Soc.*, 1961, **83**, 3373-3378.

24. E. Balboni and P. C. Burns, *J. Solid State Chem.*, 2014, **213**, 1-8.

25. T. Z. Forbes, C. Wallace and P. C. Burns, *Can. Mineral.*, 2008, **46**, 1623-1645.

26. N. N. Krot and M. S. Grigoriev, *Russian Chemical Reviews*, 2004, **73**, 89.

27. E. V. Alekseev, S. V. Krivovichev, T. Malcherek and W. Depmeier, *Inorg. Chem.*, 2007, **46**, 8442-8444.

28. A. B. Van Egmond, *J. Inorg. Nucl. Chem.*, 1976, **38**, 1645-1647.

29. SMART Version 5.631, SAINT+ Version 6.45a and SADABS Version 2.10. Bruker Analytical X-ray Systems, Inc., Madison, Wisconsin, USA, 2003.

30. G. M. Sheldrick, *Acta Crystallogr. A*, 2008, **64**, 112-122.

31. O. V. Dolomanov, L. J. Bourhis, R. J. Gildea, J. A. K. Howard and H. Puschmann, OLEX2: a complete structure solution, refinement and analysis program. *J. Appl. Crystallogr.* 2009, **42**, 339-341.

32. C. B. Hübschle, G. M. Sheldrick, and B. Bittrich, *ShelXle*: a Qt graphical user interface for *SHELXL, J. Appl. Crystallogr.* 2011, **44**, 1281-1284.

33. (a) E. Parthé and L. M. Gelato, *Acta Crysallogr.*, 1984, **A40**, 169-183 (b) L. M. Gelato and E. Parthé, *J. Appl. Crystallogr.* 1987, **20**, 139-143; (c) S.-Z. Hu and E. Parthé, *Chinese J. Struct. Chem.* 2004, **23**, 1150-1160.

34. D. Hall, A. D. Rae and T. N. Waters, *Acta Crystallogr.*, 1966, **20**, 160-162.

35. M. Aberg, *Acta Chem. Scand.*, 1969, **23**, 6.

36. M. Åberg, *Acta Chem. Scand.*, 1971, **25**, 368-369.

37. D. E. Bugaris and H.-C. zur Loye, *Angew. Chem. Int. Ed. Engl*, 2012, **51**, 3780-3811.

38. J. G. Allpress and A. D. Wadsley, *Acta Crystallogr.*, 1964, **17**, 41-46.

39. R. B. King, *Chem. Mater.*, 2002, **14**, 3628-3635.

40. P. Piret, M. Deliens, M. Piret, Jacqueline and G. Germain, *Bull. Mineral.*, 1983, **106**, 299-304.

41. L. M. Kovba, *Zh. Strukt. Khim.*, 1972, **13**, 256-259.

42. P. C. Burns, *Can. Mineral.*, 2005, **43**, 1839-1894.

43. E. V. Alekseev, S. V. Krivovichev, W. Depmeier, O. I. Siidra, K. Knorr, E. V. Suleimanov and E. V. Chuprunov, *Angew. Chem. Int. Ed.*, 2006, **45**, 7233-7235.

44. E. V. Alekseev, S. V. Krivovichev and W. Depmeier, *J. Solid State Chem.*, 2009, **182**, 2977-2984.

45. E. Balboni and P. C. Burns, *J. Solid State Chem.*, 2014, **213**, 1-8.

46. N. P. Brandenburg and B. O. Loopstra, *Acta Crystallogr. B*, 1978, **34**, 3734-3736.

47. P. M. Cantos, L. J. Jouffret, R. E. Wilson, P. C. Burns and C. L. Cahill, *Inorg. Chem.*, 2013, **52**, 9487-9495.

48. K.-A. Kubatko and P. C. Burns, *Inorg. Chem.*, 2006, **45**, 10277-10281.

49. J. Lhoste, N. Henry, P. Roussel, T. Loiseau and F. Abraham, *Dalton Trans.*, 2011, **40**, 2422-2424.

50. I. Mihalcea, N. Henry, N. Clavier, N. Dacheux and T. Loiseau, *Inorg. Chem.*, 2011, **50**, 6243-6249.

51. J. M. Morrison, L. J. Moore-Shay and P. C. Burns, *Inorg. Chem.*, 2011, **50**, 2272-2277.

52. T. A. Sullens, R. A. Jensen, T. Y. Shvareva and T. E. Albrecht-Schmitt, *J. Am. Chem. Soc.*, 2004, **126**, 2676-2677.

53. Z. Weng, S. Wang, J. Ling, J. M. Morrison and P. C. Burns, *Inorg. Chem.*, 2012, **51**, 7185-7191.

54. R. C. Severance, M. D. Smith and H.-C. zur Loye, *Inorg. Chem.*, 2011, **50**, 7931-7933.

55. C. Feldmann, *J. Solid State Chem.*, 2003, **172**, 53-58.

56. C. Y. Su, A. M. Goforth, M. D. Smith and H.-C. zur Loye, *Inorg. Chem.*, 2003, **42**, 5685-5692.

57. M. A. Tershansy, A. M. Goforth, M. D. Smith, J. Peterson, LeRoy and H.-C. zur Loye, *Acta. Crystallogr. E*, 2006, **62**, m2987-m2989.

58. P. C. Burns, R. C. Ewing and F. C. Hawthorne, *Can. Mineral.*, 1997, **35**, 1551-1570.

59. W. H. Zachariasen, *J. Less Common Metals*, 1978, **62**, 1-7.

60. P. Kubelka and F. Z. Munk, *Tech. Phys.*, 1931, **12**, 593-601.

Table 1. Crystallographic data for $K_4U_5O_{16}Cl_2$, $Rb_4U_5O_{16}Cl_2$, and $Cs_5U_7O_{22}Cl_3$.

Empirical formula	$K_4U_5O_{16}Cl_2$	$Rb_4U_5O_{16}Cl_2$	$Cs_5U_7O_{22}Cl_3$
Formula weight (amu)	1673.45	1858.93	2789.11
Crystal system	monoclinic	monoclinic	monoclinic
Space group	$P2_1/n$	$P2_1/n$	$P2_1/n$
a (Å)	9.9574(4)	10.2164(4)	10.6214(5)
b (Å)	6.9766(3)	7.0160(3)	18.1071(8)
c (Å)	14.3920(6)	14.4930(5)	16.0857(7)
β (deg)	105.7690(10)	103.8290(10)	102.9850(10)
Volume (Å^3)	962.17(7)	1008.72(7)	3014.5(2)
Z	2	2	4
ρcalc (Mg/mm^3)	5.776	6.12	6.145
μ (mm^{-1})	43.148	49.92	43.755
Temperature (K)	296(2)	296(2)	296(2)
Wavelength (Å)	0.71073	0.71073	0.71073
Final R indexes [I>=2σ (I)]	R_1 = 0.0292, wR_2 = 0.0586	R_1 = 0.0348, wR_2 = 0.0667	R_1 = 0.0409, wR_2 = 0.0734
Final R indexes [all data]	R_1 = 0.0383, wR_2 = 0.0613	R_1 = 0.0492, wR_2 = 0.0709	R_1 = 0.0628, wR_2 = 0.0808

Table 2. Crystallographic data for $RbUO_3Cl$ and $CsUO_3Cl$.

Empirical formula	$RbUO_3Cl$	$CsUO_3Cl$
Formula weight (amu)	406.95	454.39
Crystal system	monoclinic	monoclinic
Space group	$P2_1/m$	$P2_1/m$
a (Å)	7.3602(6)	7.7768(4)
b (Å)	4.1127(3)	4.1245(2)
c (Å)	8.5556(7)	8.7701(5)
β (deg)	104.602(2)	105.4680(10)
Volume (Å^3)	250.62(3)	3014.5(2)
Z	2	2
ρcalc (Mg/mm^3)	5.393	5.566
μ (mm^{-1})	42.436	36.926
Temperature (K)	296(2)	296(2)
Wavelength (Å)	0.71073	0.71073
Final R indexes [I>=2σ (I)]	R_1 = 0.0316, wR_2 = 0.0685	R_1 = 0.0256, wR_2 = 0.0563
Final R indexes [all data]	R_1 = 0.0357, wR_2 = 0.0699	R_1 = 0.0289, wR_2 = 0.0575

Table 3. Selected interatomic distances (Å) for $K_4U_5O_{16}Cl_2$, $Rb_4U_5O_{16}Cl_2$, and $Cs_5U_7O_{22}Cl_3$.

$K_4U_5O_{16}Cl_2$			$Rb_4U_5O_{16}Cl_2$			$Cs_5U_7O_{22}Cl_3$								
U1	O1	1.812(4)	U1	O1	1.803(5)	U1	O1	1.818(8)	U3	O3	2.283(7)	U6	O6	2.145(7)
	O2	1.823(4)		O2	1.828(5)		O2	1.815(8)		O4	2.220(6)		O7	2.846(7)
	O5	2.390(3)		O5	2.363(4)		O3	2.255(6)		O12	1.797(8)		O11	2.242(7)
	O5	2.294(3)		O5	2.307(4)		O4	2.449(7)		O13	1.820(9)		O18	2.549(6)
	O6	2.258(4)		O6	2.268(4)		O5	2.230(6)		O14	2.437(7)		O19	1.812(9)
	O6	2.221(3)		O6	2.235(4)		O6	2.226(6)		O15	2.758(7)		O20	1.807(8)
	O7	2.527(4)		O7	2.540(4)		O7	2.674(7)		O15	2.395(7)		O22	2.379(7)
U2	O3	1.805(4)	U2	O3	1.801(5)	U2	O5	2.282(6)	U4	O4	2.295(6)	U7	O3	2.194(6)
	O4	1.823(4)		O4	1.826(5)		O6	2.283(6)		O5	2.148(7)		O3	2.194(6)
	O5	2.186(3)		O5	2.189(4)		O8	1.798(9)		O10	2.733(7)		O14	2.324(7)
	O6	2.185(3)		O6	2.197(4)		O9	1.818(9)		O16	1.790(9)		O14	2.324(7)
	O8	2.368(3)		O8	2.372(4)		O10	2.587(7)		O17	1.814(8)		O21	1.811(9)
	O8	2.407(3)		O8	2.407(4)		O11	2.253(7)		O18	2.352(6)		O21	1.811(9)
							O11	2.362(7)		O22	2.484(7)			
U3	Cl1	2.6761(16)	U3	Cl1	2.7003(19)	U5	Cl1	2.706(3)	U8	Cl3	2.701(3)			
	Cl1	2.6761(16)		Cl1	2.7004(19)		Cl2	2.702(3)		Cl3	2.701(3)			
	O7	1.869(4)		O7	1.871(4)		O7	1.901(7)		O10	1.892(7)			
	O7	1.869(4)		O7	1.871(4)		O14	2.005(7)		O10	1.892(7)			
	O8	2.096(3)		O8	2.104(4)		O15	1.960(7)		O22	2.056(7)			
	O8	2.096(3)		O8	2.104(4)		O18	2.003(6)		O22	2.056(7)			

Table 4. Selected interatomic distances (Å) for $RbUO_3Cl$ and $CsUO_3Cl$.

		$RbUO_3Cl$	**$CsUO_3Cl$**
U1	Cl1	2.974(2)	2.9817(14)
	Cl1	2.974(2)	2.9817(14)
	O2	1.808(8)	1.802(6)
	O3	1.824(8)	1.810(6)
	O1	2.211(3)	2.214(2)
	O1	2.211(3)	2.214(2)
	O1	2.264(8)	2.268(6)

Table 5. Bond Valence Sums for $K_4U_5O_{16}Cl_2$, $Rb_4U_5O_{16}Cl_2$, $Cs_5U_7O_{22}Cl_3$, $RbUO_3Cl$, and $CsUO_3Cl$.

$K_4U_5O_{16}Cl_2$		**$Rb_4U_5O_{16}Cl_2$**		**$Cs_5U_7O_{22}Cl_3$**			
U1	6.07	U1	6.06	U1	6.00	U5	5.70
U2	5.75	U2	5.73	U2	6.06	U6	5.84
U3	5.73	U3	5.63	U3	5.80	U7	5.88
				U4	5.95	U8	5.69
		$RbUO_3Cl$		**$CsUO_3Cl$**			
		U1	5.97	U1	6.00		

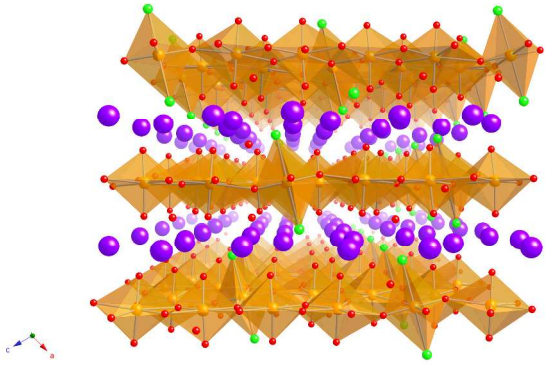

Figure 1. View of $K_4U_5O_{16}Cl_2$ down *b*, emphasizing the separation of the uranyl sheets by the alkali metal cations. Potassium, uranium, oxygen, and chlorine polyhedra/atoms are shown in violet, orange, red, and green, respectively.

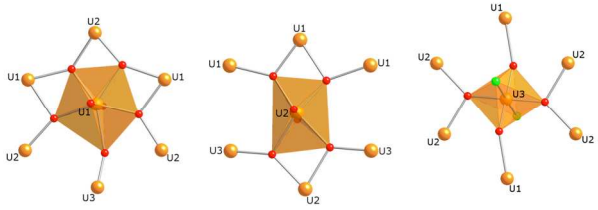

Figure 2. Polyhedral representations of the three uranium coordination environments found in $K_4U_5O_{16}Cl_2$. Uranium, oxygen, and chlorine polyhedra/atoms are shown in orange, red, and green, respectively.

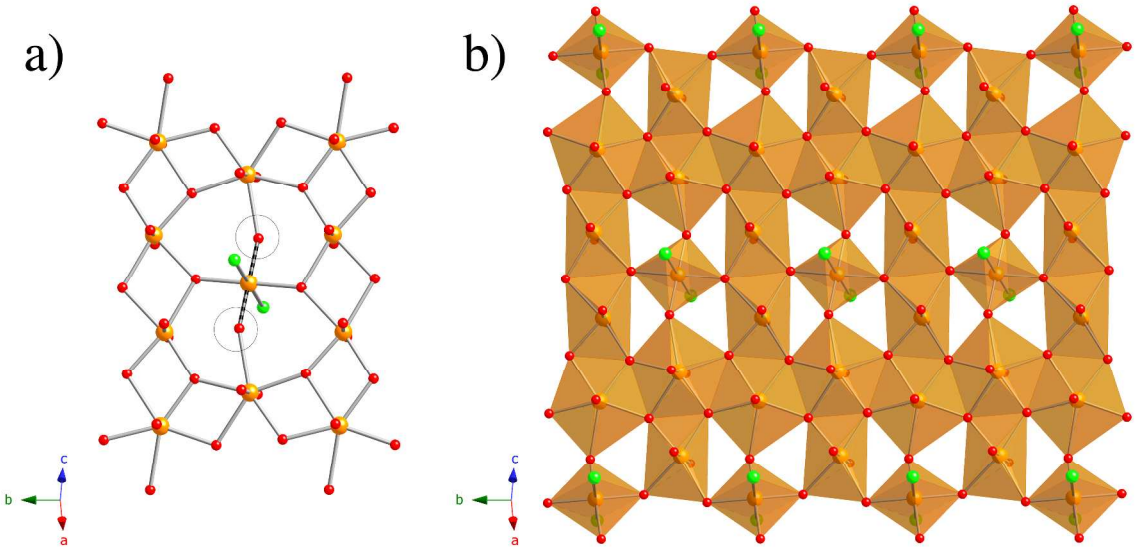

Figure 3. Top view of the uranyl sheet found in $K_4U_5O_{16}Cl_2$. a) The uranyl oxygen bond is shown with black and grey stripes with the sterically mediated CCI circled, and b) a polyhedral view. Uranium, oxygen, and chlorine polyhedra/atoms are shown in orange, red, and green, respectively.

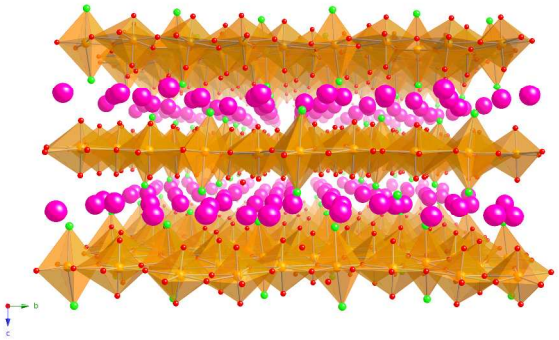

Figure 4. View of $Cs_5U_7O_{22}Cl_3$ down *a*, emphasizing the separation of the uranyl sheets by the Cs cations. Cesium, uranium, oxygen, and chlorine polyhedra/atoms are shown in pink, orange, red, and green, respectively.

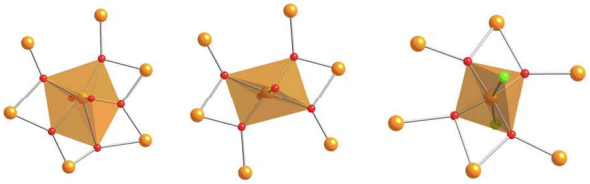

Figure 5. Polyhedral representations of the three uranium coordination environments found in $Cs_5U_7O_{22}Cl$. Uranium, oxygen, and chlorine polyhedra/atoms are shown in orange, red, and green, respectively.

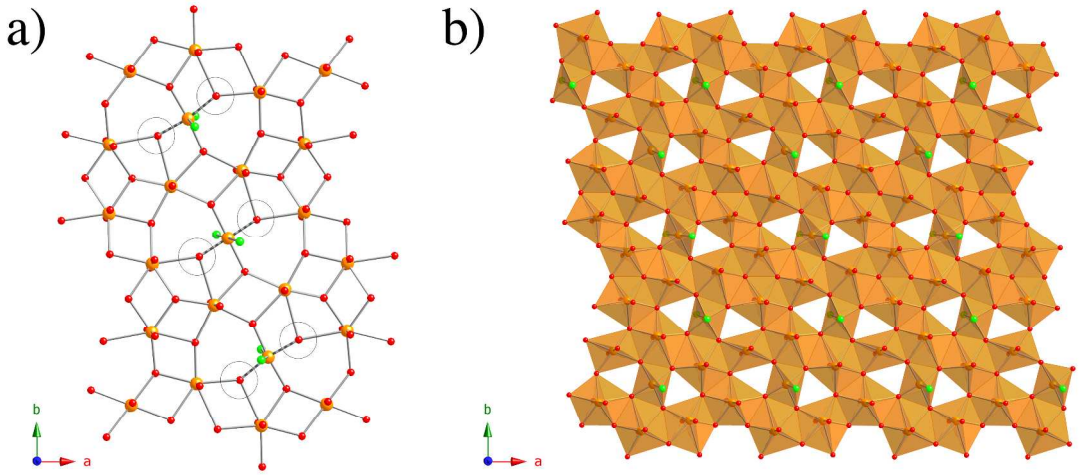

Figure 6. a) Top view of the uranyl sheet found in $Cs_5U_7O_{22}Cl_3$, with the sterically mediated CCIs circled, and b) polyhedral view of the extended sheet. Uranium, oxygen, and chlorine polyhedra/atoms are shown in orange, red, and green, respectively.

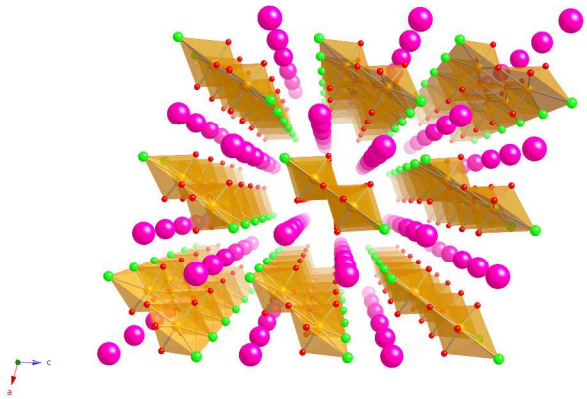

Figure 7. View of $CsUO_3Cl$ down *b*. The 1-D structure consists of double chains of edge-shared $UO_2O_3Cl_2$ polyhedra separated by respective alkali cations. Cesium, uranium, oxygen, and chlorine polyhedra/atoms are shown in pink, orange, red, and green, respectively.

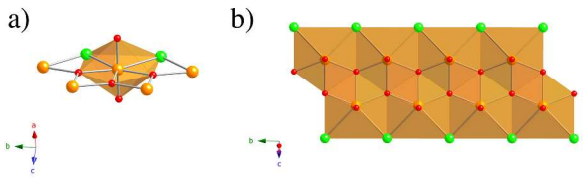

Figure 8. a) Polyhedral representation of the uranium coordination environment found in $CsUO_3Cl$, and b) top view of the zipper-like chain of edge-shared $UO_2O_3Cl_2$ polyhedra. Uranium, oxygen, and chlorine polyhedra/atoms are shown in orange, red, and green, respectively.

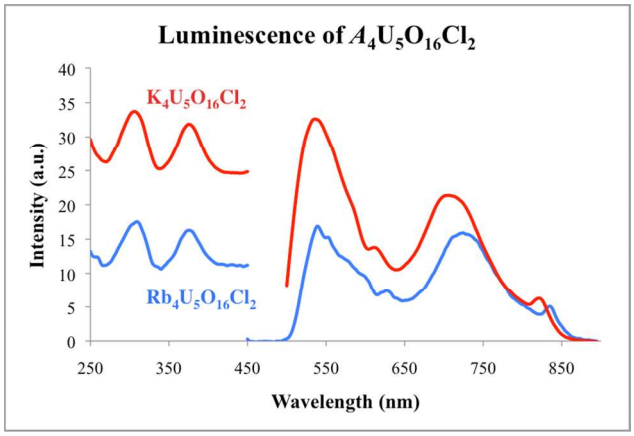

Figure 9. Luminescence data of $A_4U_5O_{16}Cl_2$. For $Rb_4U_5O_{16}Cl_2$, Em_{max} = 536 nm and Ex_{max} = 308 nm. For $K_4U_5O_{16}Cl_2$, Em_{max} = 537 nm and Ex_{max} = 311 nm.

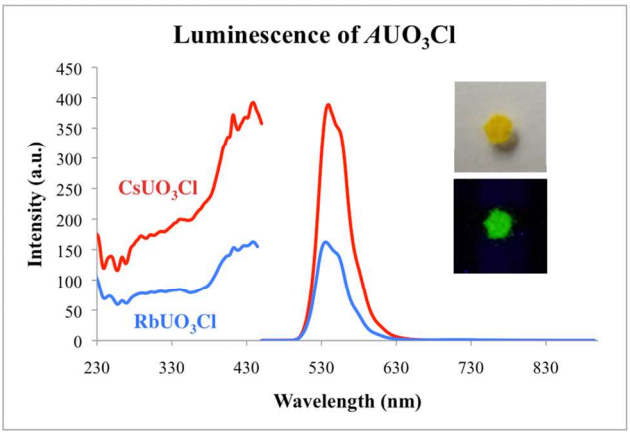

Figure 10. Luminescence data of AUO_3Cl. For $CsUO_3Cl$, Em_{max} = 539 nm and Ex_{max} = 439 nm. For $RbUO_3Cl$, Em_{max} = 535 nm and Ex_{max} = 439 nm. Inset is an optical image of $CsUO_3Cl$ crystals in fluorescent light (top) and 365 nm light (bottom).

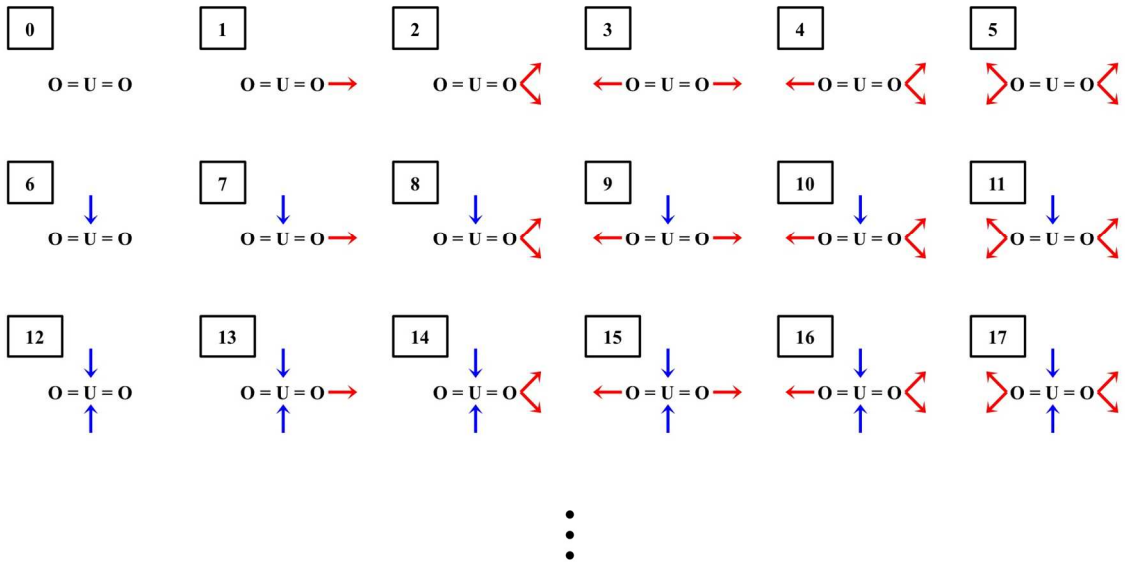

Scheme 1. Possible CCI arrangements for uranyl cations for two- and three-centered interactions. The uranyl donors and uranyl acceptors are indicated by red and blue arrows, respectively. Type **0** displays the absence of a CCI.